

Analysis of Macro-Diversity in LTE-Advanced

Gun-Yeob (Peter) Kim¹, Jung Ah C. Lee¹ and Sangjin Hong²

¹Alcatel-Lucent

Murray Hill, NJ 07974, USA

[e-mail: {peter.kim, jung.lee}@alcatel-lucent.com]

²Mobile Systems Design Laboratory

²Department of Electrical and Computer Engineering

Stony Brook University-SUNY, Stony Brook, NY 11794, USA

[e-mail: snjhong@ece.sunysb.edu]

*Corresponding author: Sangjin Hong

*Received May 4, 2010; revised July 31, 2010; January 30, 2011; accepted September 14, 2011;
published September 29, 2011*

Abstract

Coordinated Multi-Point (CoMP) transmission / reception is being studied in Long Term Evolution-Advanced (LTE-A) for future evolution of the 3rd Generation Partnership Project (3GPP) LTE. Support of soft handover is essential for improving the performance of cell edge users. CoMP provides a natural framework for enabling soft handover in the LTE system. This paper evaluates the soft handover gain in LTE-A downlink. Mathematical analysis of signal to interference plus noise ratio (SINR) gain and the handover margins for soft handover and hard handover are derived. CoMP system model is developed and an inter-cell and intra-cell interference model is derived, taking into account the pathloss, shadowing, cell loading, and traffic activity. Reference signal received power (RSRP) is used to define the triggers and the measurements for soft handover. Our results indicate that parameter choices such as handover margin and the CoMP set size impact CoMP performance gain.

Keywords: Cellular, 3GPP, LTE, coordinated multi-point transmission, macro-diversity gain

1. Introduction

3GPP LTE [1] is based on Orthogonal Frequency Division Multiple Access (OFDMA) technology. One of the main goals of LTE is to provide seamless access to voice and multimedia services with strict latency requirements which is achieved by the current technology while achieving high spectral efficiency and high peak data rate.

Hard handover is supported for the LTE systems using L3-filter, hysteresis, and time-to-trigger mechanisms [2]. CoMP transmission / reception is being studied in LTE-A [1] for further evolution of 3GPP LTE. It is foreseen that the evolution of backhaul technology can accommodate increased backhaul requirements of CoMP in LTE-A deployment timeframe. With CoMP, a user equipment (UE) at the cell edge is served by multiple sites, either by coherent or non-coherently combining the signals dynamically at the receiver. High spectral efficiency can be obtained for cell edge users. Another benefit of CoMP is the macro-diversity gain by soft handover due to the availability of the measurements from multiple base stations (BSs) along with channel state information (CSI). It is well-known that soft handover is a key technique to extend the cell coverage and to increase the cell edge user data rate in cellular communication systems [3][4]. Viterbi et al. [3] derived the effect of soft handover technique on cell coverage and reverse link capacity in the Code Division Multiple Access (CDMA) system. With soft handover, a UE in downlink receives signals from multiple BSs. The macro-diversity gain obtained by combining the signals received from multiple BSs compensate for some effect of fast channel fading and improve the communication quality [5]. K. Rege presented an analysis of handover margin for systems allowing soft handover in CDMA system [6]. In [7], hybrid handover method, termed site selection diversity transmission (SSDT) was introduced and the handover gain for OFDM-based broadband system was evaluated. Mihailescu *et al.* analyzed the behavior of the downlink soft handover and derived the macro-diversity gain in terms of SIR for W-CDMA system [8]. We extend this study to LTE-A downlink.

We analyzed the macro-diversity gain achievable by combining the signals at the UE in the LTE-A system. Our analysis is based on a simple linear topology with two evolved NodeBs (eNBs) in the CoMP set. A semi-static scheduler is assumed for downlink scheduling. The rest of this paper is organized as follows: In Section 2, we introduce the concept of CoMP set and the propagation model. In Section 3, a model for downlink interference is described. An analysis of handover margin based on the interference model is described in Section 4. Numerical results are presented in Section 5. System-level simulation results for multi-cell downlink environment are presented in Section 6. Finally, conclusions are given in Section 7.

2. CoMP Models and Assumptions

CoMP is one of the key techniques for LTE-A to improve the coverage and the cell edge user throughput. It is considered as an effective approach for inter-cell interference coordination in LTE-A. In the downlink, CoMP techniques are categorized into two methods: Coordinated Scheduling/Beamforming (CS/CB) and Joint Processing (JP) [1][9]. CB is considered as a simple solution to avoid beam collision with limited coordination among neighboring sites and either distributed or centralized scheduler can be used. JP is then subdivided into joint transmission and dynamic cell selection. Inter-site joint transmission is a type of joint processing scheme where user data is shared among the neighboring sites and is jointly

processed by multiple sites. Full channel knowledge or precoding matrix is shared among the neighboring sites. And depending on the number of users scheduled in the same time/frequency resource, inter-site Single User Multiple-Input-Multiple-Output (SU-MIMO) or inter-site Multiple User Multiple-Input-Multiple-Output (MU-MIMO) schemes are possible. In this paper, we focus on the inter-site joint transmission. This section presents the models and assumptions used to evaluate the macro-diversity gain.

2.1 CoMP Set

A regular hexagonal 19 cell layout with the reference eNB₀ and 18 neighboring eNBs is assumed in Fig. 1. CoMP cooperating set is the set of (geographically separated) points directly or indirectly participating in data transmission to the UE. The CoMP cooperating set may be determined as network-decided CoMP cooperating set or UE-specific CoMP cooperating set [10]. For the simplicity of derivation, we consider two eNBs (eNB₀ and eNB₁) as CoMP transmission points in the cooperating set. CoMP measurement set is the set of cells for which channel state information (CSI) on the link to the UE is reported. CoMP set is applicable to cell edge UEs and a handover decision on the cell edge of cells is based on the downlink received signal power.

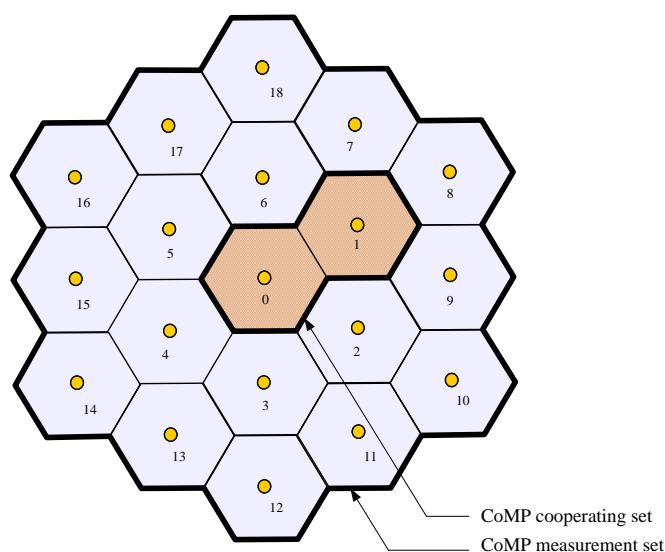


Fig. 1. CoMP system model

2.2 System Scenario

The propagation loss is generally modeled as the product of the m -th power of distance and a log-normal component representing shadowing loss. This shadowing effect is modeled as a log-normal distribution. In this paper, we only take into account the long-term propagation loss, i.e., pathloss and shadowing. Let us consider a UE located at a distance r surrounded by 18 cells in the CoMP measurement set. Then we can express the pathloss between the i -th UE ($i = 0 \dots N$) and an adjacent j -th eNB ($j = 0 \dots C$) as

$$L(i, j) = r_{i,j}^{-m} 10^{\xi_{i,j}/10} \quad (1)$$

where m is the pathloss exponent, $r_{i,j}$ is the distance between the i -th UE and j -th eNB, and $\zeta_{i,j}$ is the attenuation in dB due to shadow fading which is modeled as a zero-mean Gaussian random variable with standard deviation σ_{SH} . Empirical data show that $m = 4$ and $\sigma_{SH} = 8$. Considering the dependence of the shadow fading of different eNBs, $\zeta_{i,j}$ is expressed as the weighted sum of a component ζ which is in the near field of the user that is common to all eNBs and a component $\zeta_{i,j}$ which is independent from one eNB to another.

Thus, the random component of the received signal at eNB can be expressed as $\zeta_{i,j} = a\zeta + b\zeta_{i,j}$ where $a^2 + b^2 = 1$ [4]. In our analysis, the propagation model accommodates shadow correlation between the two eNBs, j and l ($j, l = 0, 1, 2, \dots, C$). The correlation coefficient is given by

$$\frac{E(\zeta_j \zeta_l)}{\sigma_{SH}^2} = a^2 = 1 - b^2 (j \neq l) \quad (2)$$

Assuming identical standard deviations for propagation, $a^2 = b^2 = 0.5$ and the normalized covariance is 0.5 for all pairs of eNBs. Both components are assumed to be Gaussian distributed random variables with zero-mean and standard deviation σ_{SH} [3]. We consider two CoMP transmission points in the cooperating set where a UE $_i$ on a straight line joining reference eNB $_0$ and neighboring eNB $_1$ as shown in Fig. 2.

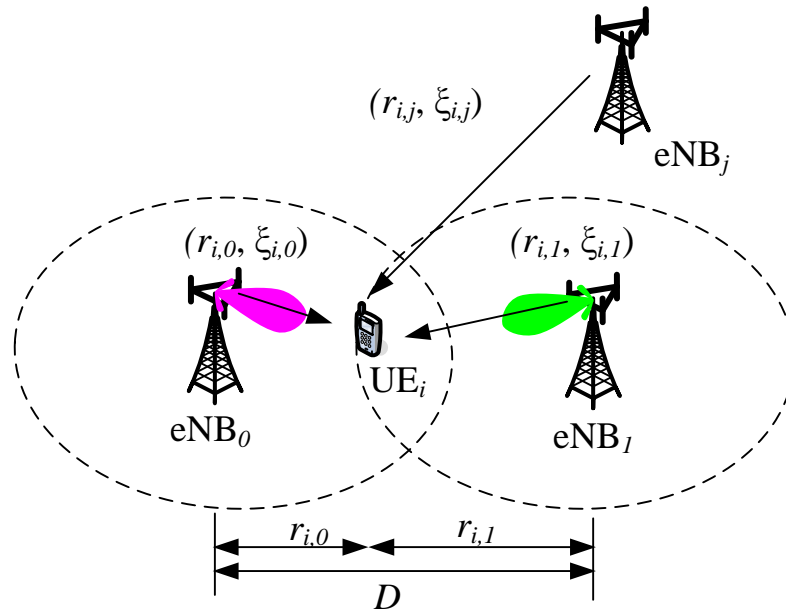


Fig. 2. System Model

3. Downlink Interference Analysis

To evaluate the SINR, interference modeling is required. The total interference (I_{tot}) experienced by the UE is composed of two parts: intra-cell (I_{intra}) and inter-cell interference (I_{inter}). The generalized expression for the SINR of a UE $_i$ which is connected to eNB $_j$ can be expressed as

$$\begin{aligned}
SINR_{i,j}^{user} &= \frac{C_{i,j}}{I_{intra,i,j} + I_{inter,i,j} + N_0} \\
&= \left(\frac{I_{intra,i,j}}{C_{i,j}} + \frac{I_{inter,i,j}}{C_{i,j}} + \frac{N_0}{C_{i,j}} \right)^{-1}
\end{aligned} \tag{3}$$

where N_0 is thermal noise per user including UE noise figure, $C_{i,j}$ is the received signal power from eNB_{*j*}. Taking expectations from (3) and by Jensen's inequality for convex function, we obtain

$$E[SINR_{i,j}^{user}] \geq \left(E\left[\frac{I_{intra,i,j}}{C_{i,j}}\right] + E\left[\frac{I_{inter,i,j}}{C_{i,j}}\right] + \left[\frac{N_0}{C_{i,j}}\right] \right)^{-1} \tag{4}$$

3.1 Intra-cell Interference

The intra-cell interference to a certain UE comes from its serving eNB and caused by inter-carrier interference (ICI). Inter-carrier interference is generated due to frequency mismatch between the UEs. The ICI_{*i*} in **Fig. 3(a)** is the inter-carrier interference which can be generated at resource blocks for user *i* and only carriers at the border may impact neighboring UEs.

Assuming a simple semi-static scheduling strategy to serve the user with equal data rates and same Modulation and Coding Scheme (MCS) selection for each user, the number of frequency resources allocated to each user is identical. The total transmitted power in the downlink at serving eNB_{*0*} is

$$P_{tot_0} = \sum_{i=0}^N P_{i,0} \tag{5}$$

where, $P_{i,0}$ is the transmitted power to the *i*-th UE from the serving eNB_{*0*}. The total transmitted power is equally divided among all the UEs in the cell. The intra-cell interference $I_{intra,i,0}$ to the *i*-th UE can be simply expressed as $P_{tot_0} \times L(i,0)$. Here, $L(i,0)$ is the pathloss between UE_{*i*} and eNB_{*0*}. We extend the analysis to see the effects of N_{tot} , δ , and ε on SINR. Here, N_{tot} is the total number of users in the cell, δ is the traffic channel activity factor, and ε is the intra-cell interference coefficient, which is a fraction of intra-cell interference to total transmit power.

Fig. 3(a) illustrates the semi-static scheduler principle and the inter-carrier interference for UE_{*i*} assuming a semi-static scheduler. With this assumption, the loading denoted as ρ_0 is the fraction of used physical resource blocks (PRBs) [11] occupied by each UE in eNB_{*0*} and is written as

$$\rho_0 = \frac{N_{used}^{PRB}}{N_{tot}^{PRB}} \tag{6}$$

The amount of intra-cell interference is derived as

$$I_{intra,i,0} = \varepsilon \delta \frac{\rho_0 P_{tot_0}}{N_{tot}} L(i, 0) \quad (7)$$

The traffic activity factor can be controlled by eNB by suitable control mechanisms depending on buffer occupancy and the user throughput. Consequently, from (3) and (7), we obtain the intra-cell interference to signal portion of the SINR equation

$$\frac{I_{intra,i,0}}{C_{i,0}} = \frac{\varepsilon \delta \rho_0 P_{tot_0} L(i, 0) / N_{tot}}{\rho_0 P_{tot_0} L(i, 0) / N_{tot}} = \varepsilon \delta \quad (8)$$

Fig. 3(b) shows an example of user resource allocation in eNBs associated with **Fig. 3(c)**. We assume that UE_i ($i=0,1,2,3,4,5$) are located in neighboring eNB $_j$ ($j = 0,1,2$). Assuming that each eNB transmits data at the assigned resource blocks simultaneously, the intra-cell interference to UE_0 is due to the resource blocks of UE_1 and UE_2 that are adjacent to UE_0 . **Fig. 3(c)** shows the multi-point transmission where we assume that two eNBs are selected for CoMP joint transmission. As indicated by the blue arrows in the figure, the intra-cell interference from UE_1 and UE_2 scheduled in the neighbor PRBs is negligible. The intra-interference is dominated by the portion of the resource blocks allocated to UE_0 .

Note that (8) is a function of ε and δ only and is independent of UE location and the number of UEs. This means that we only need to consider UE_i (for example, UE_0 in **Fig. 3(c)**) in eNB $_0$ for intra-cell interference analysis.

3.2 Inter-cell Interference

To a UE linked to eNB $_j$, the inter-cell interference is the power received by UE from all other eNBs around it except its serving eNB $_0$. Inter-cell interference, with eNB $_0$ being the serving cell for UE_i is obtained as

$$I_{inter,i,j} = \delta \sum_{j=1}^c \frac{\rho_j P_{tot_j}}{N_{tot}} L(i, j) \quad (9)$$

We assume that the number of users and the cell loading is equal in all eNBs and the eNB transmitted power is identical. Then we obtain the inter-cell interference to signal portion of the SINR equation

$$\begin{aligned} \frac{I_{inter,i,j}}{C_{i,0}} &= \frac{\delta \sum_{j=1}^c \rho_j P_{tot_j} L(i, j) / N_{tot}}{\rho_0 P_{tot_0} L(i, 0) / N_{tot}} \\ &= \delta \frac{\sum_{j=1}^c L(i, j)}{L(i, 0)} = \delta \sum_{j=1}^c \left(\frac{r_{i,0}}{r_{i,j}} \right)^m 10^{(\xi_{i,j} - \xi_{i,0})/10} \end{aligned} \quad (10)$$

Fig. 3(b) shows an example of user resource allocation in eNBs. The inter-cell interference

to UE_0 is due to interference from neighbor cell UEs scheduled in the same PRBs as UE_0 . For this reason, the interference is characterized by narrow band interference unlike CDMA/W-CDMA systems. **Fig. 3(c)** illustrates the multi-point transmission where two eNBs are selected for CoMP joint transmission. The red arrows show that the signals from eNB_1 to UE_3 and from eNB_2 to UE_4 do not cause intra-cell interference to UE_0 . The case that only causes inter-cell interference is indicated by the green arrow where the eNB_2 transmits signals to UE_5 scheduled in the same PRBs as UE_0 .

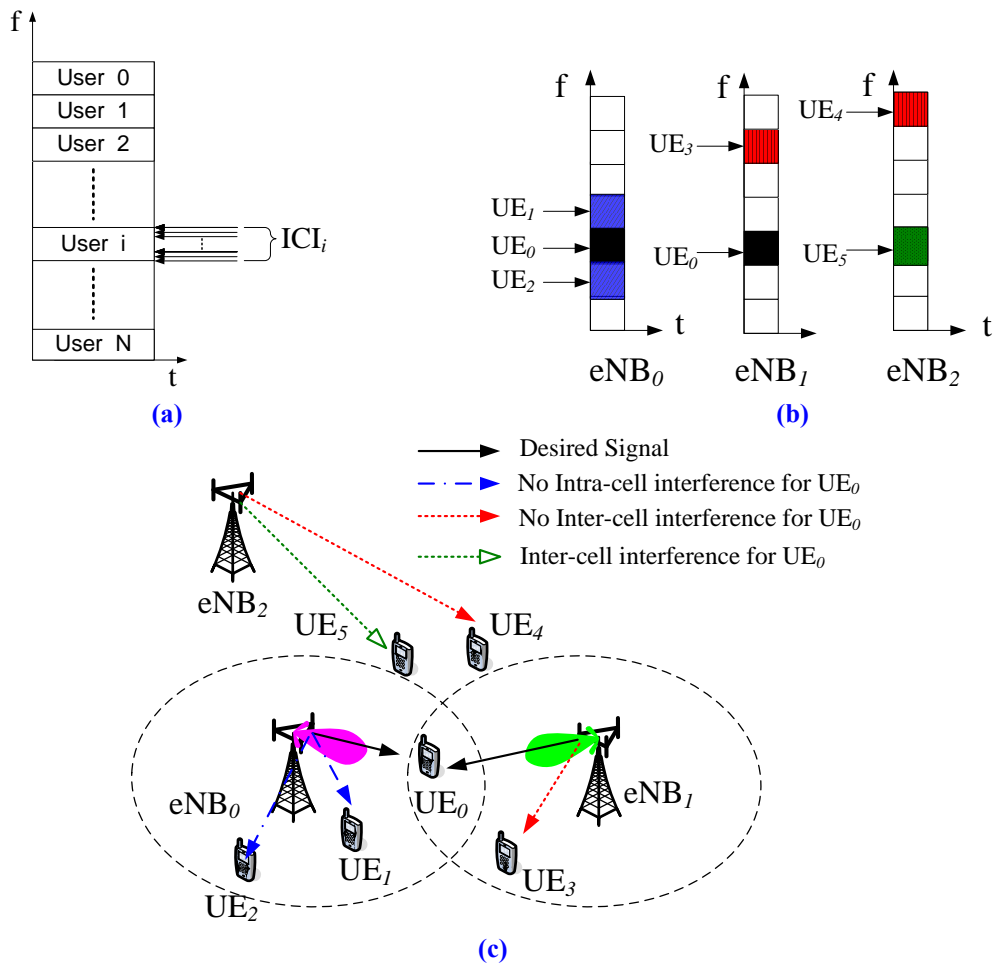


Fig. 3. Assumption for interference analysis (a) Resource allocation by semi-static scheduler (b) Example of user allocation in eNBs and (c) Multi-point reception and inter-cell interference model

4. Analysis of Hard and Soft Handovers

In this section, we analyze the soft handover gain by evaluating the handover (HO) gain. The two key design parameters are CoMP set size and the handover margin. The handover gain also depends on the UE receiver processing. Maximal Ratio Combining (MRC) is assumed in this paper.

4.1 Hard Handover Analysis

For hard handover, RSRP of a single cell is tracked at any one time instance. To avoid the “ping-pong” effect, handover is allowed when the second cell’s RSRP is sufficiently higher than that of the first. This margin is called “handover margin.”

The probability P_0 that UE_{*i*} is only served by eNB₀ is [12]

$$\begin{aligned}
 P_0 &= \text{Prob}\left[RSRP_0 > RSRP_1 + M_{SH}\right] \\
 &= \frac{1}{\sqrt{2\pi}} \int_{\frac{10m \log(r_{i,0}/r_{i,1}) + M_{SH}}{b}}^{\infty} \frac{\exp(-x^2 / 4b^2\sigma^2)}{\sqrt{2b\sigma}} dx \\
 &= Q\left(\frac{10m \log(r_{i,0}/r_{i,1}) + M_{SH}}{\sqrt{2b\sigma}}\right) \\
 &= Q\left(\frac{M_{i,0} - M_{i,1} + M_{SH}}{\sqrt{2b\sigma}}\right)
 \end{aligned} \tag{11}$$

where M_{SH} is the soft handover margin, $M_{i,j}$ is defined as $10m \log r_{i,j}$, and the Q -function can be expressed as [13]

$$Q(x) = \frac{1}{\sqrt{2\pi}} \int_x^{\infty} \exp^{-z^2/2} dz \tag{12}$$

In order to calculate $E[SINR_{i,0}^{user}]$, we first compute the expectation value of (8) as

$$E\left[\frac{I_{intra_{i,0}}}{C_{i,0}}\right] = \varepsilon\delta \tag{13}$$

Then we calculate the expectation value of (10). From (10), the mathematical expectation can be expressed as the integral of the probability density function of the log-normal Gaussian random variable. Thus (10) can be expressed as a Q -function

$$\begin{aligned}
 E\left[\frac{I_{inter_{i,j}}}{C_{i,0}}\right] &= \delta \sum_{j=1}^C \left(\frac{r_{i,0}}{r_{i,j}}\right)^m E\left[10^{(\xi_{i,j} - \xi_{i,0})/10}; RSRP_0 > RSRP_j + M_{SH}\right] \\
 &= \delta \sum_{j=1}^C \left(\frac{r_{i,0}}{r_{i,j}}\right)^m e^{(\beta\sigma)^2/2} Q\left(\beta\sigma + \frac{10m \log(r_{i,0}/r_{i,j}) + M_{SH}}{\sigma}\right) \\
 &= \delta e^{(\beta\sigma)^2/2} \sum_{j=1}^C \left(\frac{r_{i,0}}{r_{i,j}}\right)^m Q\left(\beta\sigma + \frac{M_{i,0} - M_{i,j} + M_{SH}}{\sigma}\right)
 \end{aligned} \tag{14}$$

where $\xi_{i,j} - \xi_{i,0} = b(\zeta_{i,j} - \zeta_{i,0})$ is a zero-mean Gaussian random variable and $\beta = \ln(10)/10$. As is shown in Fig. 2, the parameter $r_{i,0}$ is the distance of UE_{*i*} from the serving eNB₀. Let us assume that the UE location follows a simple linear topology between eNB₀ and eNB₁. In the

following analysis, the distance $r_{i,0}$ is normalized relative to the distance D between eNB₀ and eNB₁. Due to symmetry, the range between 0.1 and 0.5 will be considered in the numerical analysis of SINR.

Using (13) and (14), $E[\text{SINR}_{i,0}^{user}]$ for UE_{*i*} served only by eNB₀ can be calculated from (4). Similarly, the probability P_I that UE_{*i*} is only served by eNB₁ and the corresponding SINR $E[\text{SINR}_{i,1}^{user}]$ can be derived from the same formula.

4.2 Soft Handover Analysis

With 2-way soft handover, desired signal from the two active eNBs in CoMP set are combined together whereas the signals from the rest of the eNBs are considered as interferences. MRC is assumed in this paper. We can derive the probability P_{0I} that the UE_{*i*} is connected to two eNBs simultaneously in the CoMP cooperating set as [12]

$$\begin{aligned} P_{0I} &= \text{Prob}(RSRP_1 - M_{SH} < RSRP_0 < RSRP_1 + M_{SH}) \\ &= Q\left(\frac{M_{i,0} - M_{i,1} - M_{SH}}{\sqrt{2b\sigma}}\right) - Q\left(\frac{M_{i,0} - M_{i,1} + M_{SH}}{\sqrt{2b\sigma}}\right) \end{aligned} \quad (15)$$

From (10), we obtain

$$\begin{aligned} E\left[\frac{I_{inter,j}}{C_{i,0}}\right] &= \delta \left(\frac{r_{i,0}}{r_{i,1}}\right)^m E[10^{(\xi_{i,j} - \xi_{i,0})/10}; RSRP_1 - M_{SH} < RSRP_0 < RSRP_1 + M_{SH}] \\ &+ \delta \sum_{j=2}^C \left(\frac{r_{i,0}}{r_{i,j}}\right)^m E[10^{(\xi_{i,j} - \xi_{i,0})/10}; RSRP_0 > RSRP_j + M_{SH}] \end{aligned} \quad (16)$$

Again, (16) can be rewritten as

$$\begin{aligned} E\left[\frac{I_{inter,j}}{C_{i,0}}\right] &= \delta e^{(\beta\sigma)^2/2} Q\left(\beta\sigma + \frac{M_{i,0} - M_{i,1} - M_{SH}}{\sigma}\right) - \delta e^{(\beta\sigma)^2/2} Q\left(\beta\sigma + \frac{M_{i,0} - M_{i,1} + M_{SH}}{\sigma}\right) \\ &+ \delta e^{(\beta\sigma)^2/2} \sum_{j=2}^C \left(\frac{r_{i,0}}{r_{i,j}}\right)^m Q\left(\beta\sigma + \frac{M_{i,0} - M_{i,j} + M_{SH}}{\sigma}\right) \end{aligned} \quad (17)$$

With macro-diversity combining, the eNB₀ and eNB₁ are the actual serving cells to UE_{*i*} in soft handover, while the remaining neighboring eNBs are considered interfering cells. Using (13) and (17), the $E^*[\text{SINR}_{i,0}^{user}]$ for UE_{*i*} located when it is served by eNB₀ can be calculated from (4).

Similarly, the $E^*[\text{SINR}_{i,1}^{user}]$ for UE_{*i*} when it is served by eNB₁ can be derived from same formula.

Let $E^*[\text{SINR}_{i,01}^{user}]$ denote the SNR with MRC in soft handover between eNB₀ and eNB₁. It is given by

$$E^*[\text{SINR}_{i,01}^{user}] = E^*[\text{SINR}_{i,0}^{user}] + E^*[\text{SINR}_{i,1}^{user}] \quad (18)$$

From (4), the SINR with MRC is obtained as

$$\begin{aligned}
E^*[SINR_{i,01}^{user}] &= E^*[SINR_{i,0}^{user}] + E^*[SINR_{i,1}^{user}] \\
&= \left(E\left[\frac{I_{intra_{i,0}}}{C_{i,0}}\right] + E\left[\frac{I_{inter_{i,j}}}{C_{i,0}}\right] + \left[\frac{N_0}{C_{i,0}}\right] \right)^{-1} + \left(E\left[\frac{I_{intra_{i,1}}}{C_{i,1}}\right] + E\left[\frac{I_{inter_{i,j}}}{C_{i,1}}\right] + \left[\frac{N_0}{C_{i,1}}\right] \right)^{-1} \\
&= \left(\varepsilon\delta + \delta e^{(\beta\sigma)^2/2} Q\left(\beta\sigma + \frac{M_{i,0} - M_{i,1} - M_{SH}}{\sigma}\right) - \delta e^{(\beta\sigma)^2/2} Q\left(\beta\sigma + \frac{M_{i,0} - M_{i,1} + M_{SH}}{\sigma}\right) \right)^{-1} \\
&\quad + \left(\delta e^{(\beta\sigma)^2/2} \sum_{j=2}^C \left(\frac{r_{i,0}}{r_{i,j}}\right)^m Q\left(\beta\sigma + \frac{M_{i,0} - M_{i,j} + M_{SH}}{\sigma}\right) + \left[\frac{N_0}{C_{i,0}}\right] \right)^{-1} \\
&\quad + \left(\varepsilon\delta + \delta e^{(\beta\sigma)^2/2} Q\left(\beta\sigma + \frac{M_{i,1} - M_{i,0} - M_{SH}}{\sigma}\right) - \delta e^{(\beta\sigma)^2/2} Q\left(\beta\sigma + \frac{M_{i,1} - M_{i,0} + M_{SH}}{\sigma}\right) \right)^{-1} \\
&\quad + \left(\delta e^{(\beta\sigma)^2/2} \sum_{j=2}^C \left(\frac{r_{i,1}}{r_{i,j}}\right)^m Q\left(\beta\sigma + \frac{M_{i,1} - M_{i,0} + M_{SH}}{\sigma}\right) + \left[\frac{N_0}{C_{i,1}}\right] \right)^{-1}
\end{aligned} \tag{19}$$

Thus, the average SINR with macro-diversity is obtained as

$$E[SINR_{i,total}^{user}] = P_0 E[SINR_{i,0}^{user}] + P_{01} E^*[SINR_{i,01}^{user}] + P_1 E[SINR_{i,1}^{user}] \tag{20}$$

5. Numerical Analysis

A numerical analysis was carried out using the SINR expressions derived in the previous sections. The effect of system parameters on the SINR performance is evaluated for the scenario described in section 2.2. In this analysis, the parameters are defined in [Table 1](#).

Table 1. Parameters in numerical results

Parameter	Definition
$r_{i,0}$	Distance between serving eNB ₀ and UE ₀
D	Inter-site distance (ISD) between serving eNB ₀ and neighbor eNB ₁
$r_{i,0}/D$	Normalized distance between the UE and eNB ₀
δ	Traffic channel activity factor
m	Pathloss exponent
σ_{SH}	Standard deviation of shadow fading (in dB)
ε	Intra-cell interference coefficient
M_{SH}	Soft handover margin

The performance of soft handover is compared with hard handover in terms of SINR gain under different simulation conditions, by varying the parameters M_{SH} , m , ε , and σ_{SH} . The macro-diversity combining is obtained by setting the soft handover margin M_{SH} to a non-zero value, while $M_{SH} = 0$ means hard handover. The SINR performance can be improved significantly by properly setting the soft handover margin as can be observed in the following numerical results. In [Fig. 4](#), the SINR versus distance $r_{i,0}/D$ for different values of M_{SH} is shown. We considered $\delta = 0.5$ and $m = 3$. The X-axis defines the normalized distance in the

range from 0.1 to 0.9, where 0.5 means the cell border. When M_{SH} is changed from 0 to 2 dB, and from 2 dB to 4 dB, the SINR at the cell border is increased by 1.8 dB and 1.2 dB, respectively.

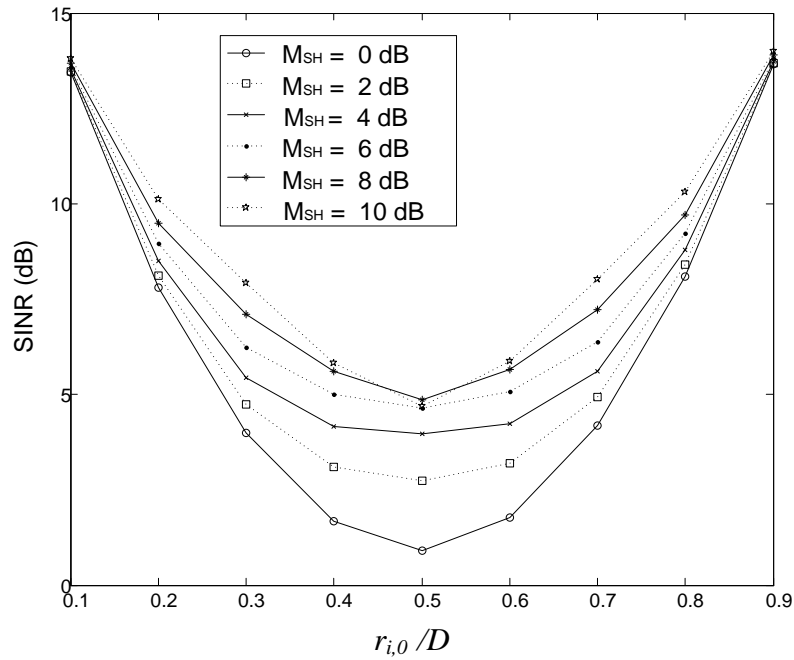


Fig. 4. SINR depending on distance $r_{i,0}/D$ ($m = 3$, $\sigma_{SH} = 8$ dB, and $\varepsilon = 0.05$)

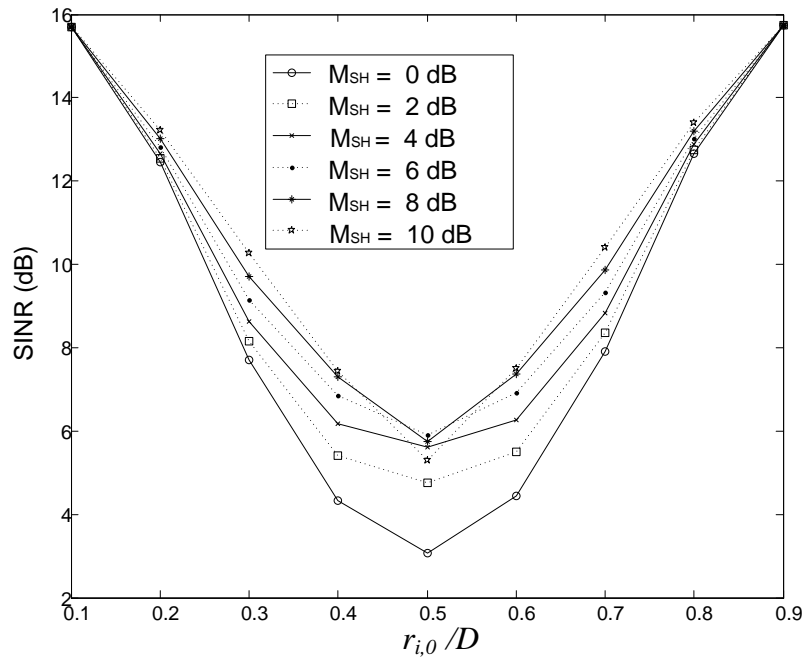


Fig. 5. SINR depending on distance $r_{i,0}/D$ ($m = 4$, $\sigma_{SH} = 8$ dB, and $\varepsilon = 0.05$)

Fig. 5 shows the SINR when m is increased from 3 to 4. Compared with Fig. 4, the result

shows that the gain in SINR is about 2 dB. This is due to inter-cell interference reduction due to increased path loss for signals coming from the neighboring cells.

In **Fig. 6**, we show the SINR as the intra-cell interference factor ε is varied. As we observed in the previous section, the parameter ε directly affects the intra-cell interference and HO performance. The figure shows that the SINR improves as ε becomes smaller, due to decreased intra-cell interference. The effect of intra-cell interference on SINR is larger for large values of M_{SH} relative to the inter-cell interference, resulting in larger difference in SINR values. It is also observed that the SINR becomes saturated when $M_{SH} = 6$ dB. The reason is that for larger values of SHO margin, most UEs will have single transmission points and will not benefit from macro diversity.

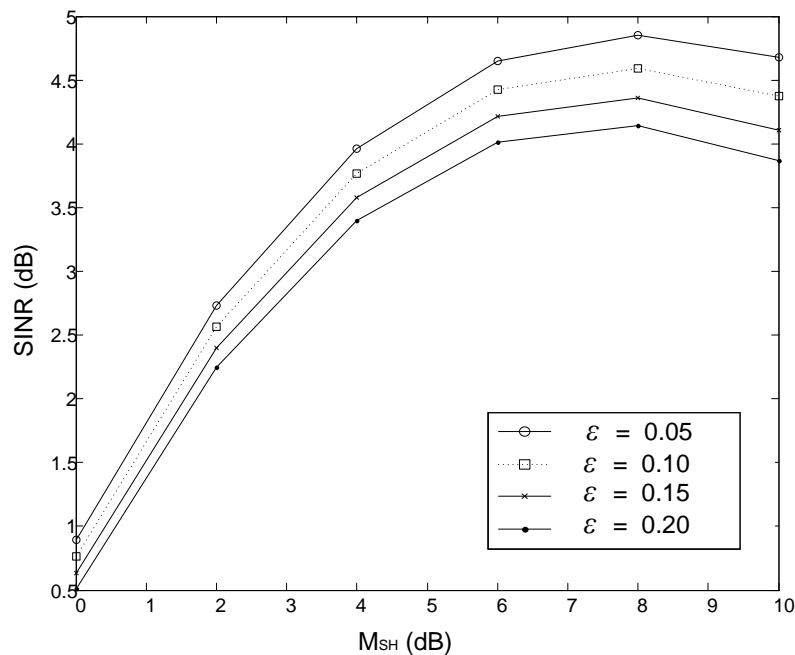


Fig. 6. SINR versus M_{SH} for different values of ε (distance $r_{i,0}/D = 0.5$)

We can emphasize the importance of the propagation parameters for the soft handover performance. We evaluate the SINR with respect to the choice of parameters m and σ_{SH} . **Fig. 7** shows the effect of pathloss exponent m on the SINR with the soft handover margin of 0 to 10. The SINR increases as the M_{SH} is increased from 0 to 4 dB. The SINR improves significantly when m increases due to inter-cell interference reduction. This behavior was also observed in **Fig. 4** and **Fig. 5**.

In **Fig. 8**, the SINR versus M_{SH} is shown for different values σ_{SH} . The dynamic range of the SINR changes by 0.5 dB to 2 dB when M_{SH} increases from 0 to 10 dB respectively. It is interesting to note that the SINR with higher M_{SH} is increased considerably as the σ_{SH} is increased since the large differences of two received signal power leads the higher combining gain.

As we observed in the analysis above, the SINR has the largest gain when M_{SH} is changed from 0 to 2 dB, where $M_{SH} = 0$ means hard handover. The result shows that soft handover with macro-diversity provides significant gain on the downlink SINR compared with hard handover. The SINR gain with soft handover is also achieved when M_{SH} is changed from 2 dB to 4 dB and from 4 dB to 6 dB. Although the SINR improves as M_{SH} increases, it will cause the

capacity issue in the network. Thus, we further evaluated the system-level performance in multi-cell, multi-user environment in Section 6.

The results studied could be applied to system design and deployment, where SINR gain can be achieved by optimizing M_{SH} , depending on propagation condition.

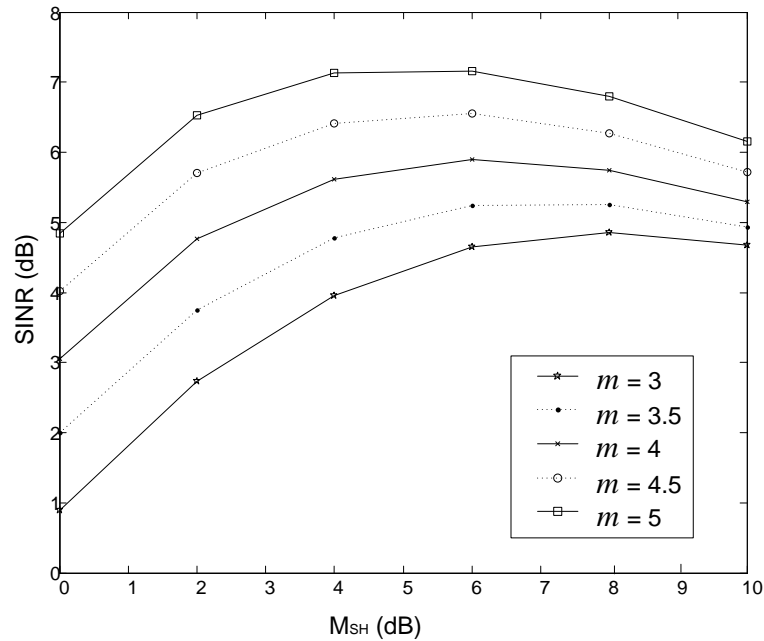


Fig. 7. SINR versus M_{SH} for different values of pathloss exponent m (distance $r_{i,0}/D = 0.5$)

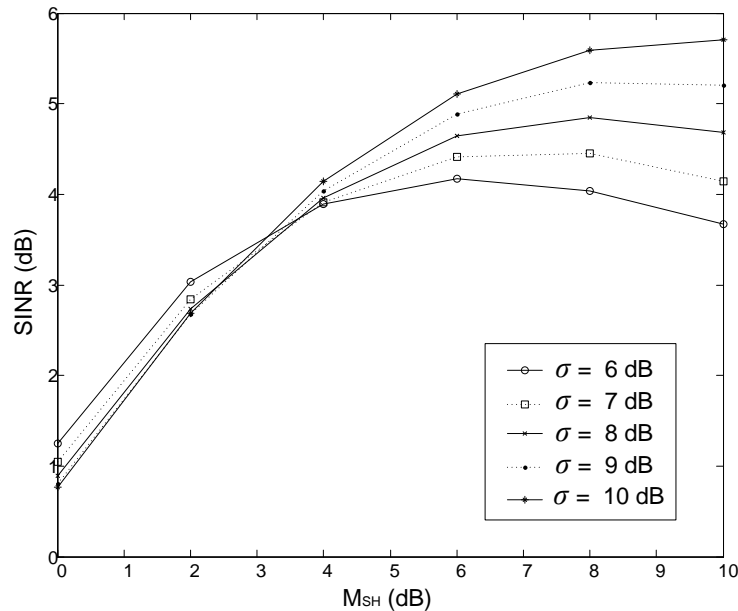


Fig. 8. SINR versus M_{SH} for different values of σ_{SH} (distance $r_{i,0}/D = 0.5$)

6. System-Level Simulation Results

In order to determine the handover margin M_{SH} for CoMP set selection and the optimum number of cells in the CoMP set, system-level simulation is set up with 57 cells. The macro cell deployment is considered with 32 UEs dropped randomly. The details of simulation parameters are summarized in **Table 2**.

Table 2. Simulation parameters

Parameters	Definition
Cellular Layout	Hexagonal grid, 19 sites, 3 sectors per site
User	33 UEs per sector
ISD	500 m
Distance-dependent path loss	$128.1+37.6\log_{10}(R)$, R in km
Lognormal Shadowing with shadowing standard deviation	8 dB (6, 7, 9 and 10 dB)
Shadowing correlation between cells	0.5
Shadowing correlation between sectors	1.0
Penetration Loss	20 dB
eNB Tx Power	46 dBm
UE Tx Power	23 dBm
eNB antenna gain	14 dBi
UE antenna gain	0 dBi
Antenna height at the eNB	32 m
Antenna height at the UE	1.5 m
UE speed	3 km/h

We considered 2 cases in this study. In the first set of analysis, the percentage of CoMP UEs depending on M_{SH} was analyzed. Different values of M_{SH} from 0 to 10 dB are simulated for $\sigma_{SH} = 6, 7, 8, 9,$ and 10 dB respectively. In **Fig. 9**, the percentage of UEs in the CoMP set as a function of M_{SH} is plotted. The plot shows that the probability of CoMP UEs (which are in the soft handover area) increase as M_{SH} increases. The results for different values of σ_{SH} show similar trends with a small variance. For M_{SH} values of 2 dB to 4 dB, the percentage of CoMP UEs in a cell increases from 15% to 35% respectively. Larger values of M_{SH} can improve the SINR of CoMP UEs at the cell edge due to higher diversity gain. However, as M_{SH} increases, cell throughput decreases. Increased resource consumption for the CoMP UEs outweighs the macro-diversity gain. The optimum value of M_{SH} needs to be determined taking into account the trade-off between the edge user data rate and the overall cell throughput.

In the second set of analysis, the probability of the number of cells within a margin depending on M_{SH} and the probability of N-way Soft handover are analyzed. For planning of a large LTE-A network, it is necessary to determine the size of CoMP set such that an upper bound for the network capacity is maintained. Here, interest is how to determine the CoMP set size and how the choice of M_{SH} influences the result. The CDF of number of cells with signal strengths within M_{SH} is listed in **Table 3**. In this table, probabilities are 98% and 91% in case of $M_{SH} = 2$ dB and 4 dB, respectively. Thus as we observed in **Fig. 9**, a reasonable size of CoMP cooperation set is 3 in case of $M_{SH} = 2$ dB and 4 dB. In **Table 4**, more detail analysis is performed. This results show the probabilities of N-way soft handover. When $M_{SH} = 2$ dB and 4 dB, the probabilities of N-way soft handover are 99.2% and 98.2%, respectively. This result also shows that the percentage of N-way soft handover with $N > 3$ is less than 2%.

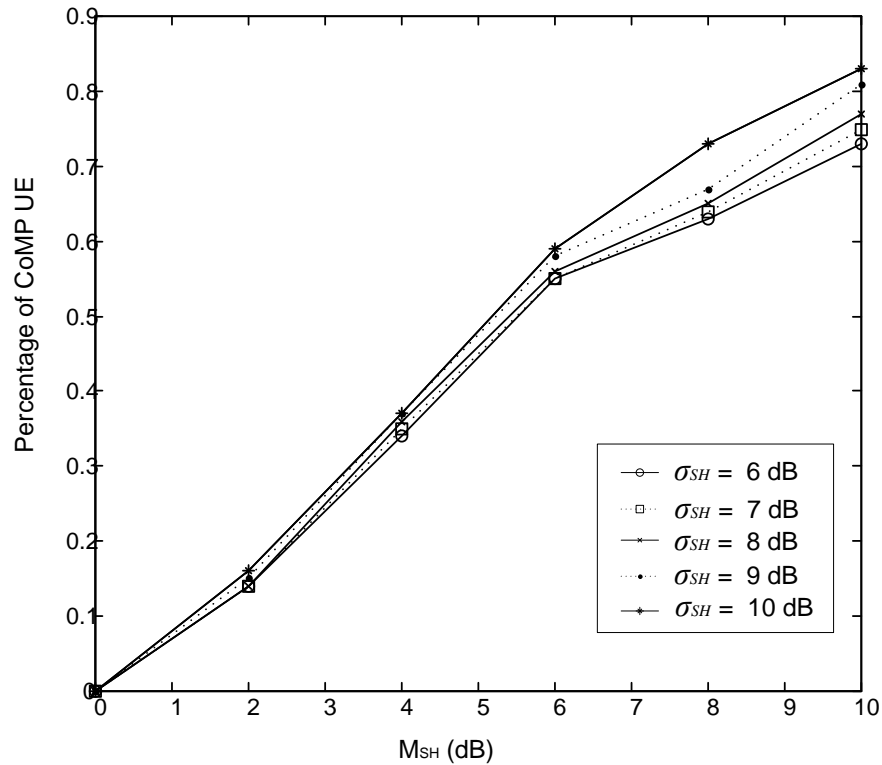


Fig. 9. Percentage of CoMP UE versus M_{SH} for different values of σ_{SH}

In this simulation, we evaluated the gain of soft handover over hard handover by system-level simulation. Although any value of soft handover margin of 2 dB, 4 dB, or 6 dB is a good choice for SINR performance, the simulation results show that 6 dB threshold consumes too much network resource unless otherwise required for specific region. Overall, $M_{SH} = 2$ dB, 3 dB, or 4 dB shows improved soft handover performance in system-level simulation result and, which is consistent with the numerical result described in Section 5.

Table 3. Probability of number of cells depending on M_{SH}

Number of cells within M_{SH}	The Probability of having $\leq N$ cells in the CoMP Set [%]					
	$M_{SH} = 0$	$M_{SH} = 2$	$M_{SH} = 4$	$M_{SH} = 6$	$M_{SH} = 8$	$M_{SH} = 10$
1	0	72.1	53.2	38.0	28.6	23.8
2	0	93.8	80.1	63.9	52.3	44.3
3	0	98.5	91.0	79.4	66.6	58.2
4	0	99.6	96.4	88.6	76.6	66.9
more than 5	0	100	100	100	100	100

Table 4. Probability of N-way soft handover

Number of cells connected to UE	The probabilities of N-way soft handover [%]					
	$M_{SH} = 0$	$M_{SH} = 2$	$M_{SH} = 4$	$M_{SH} = 6$	$M_{SH} = 8$	$M_{SH} = 10$
1	100	81.5	75.2	60.2	49	42
2	-	15.6	18.2	23.4	27.8	25.3
3	-	2.1	4.8	10.2	12.5	14.1
4	-	0.7	1.3	3.9	4.2	5.2
5	-	0	0.2	1.3	3.2	4.8

6	-	0.1	0.3	0.4	1.5	3.7
7	-	-	-	0.4	0.9	1.9
8	-	-	-	0.1	0.6	1.4
9	-	-	-	0	0	0.8
10	-	-	-	0.1	0.3	0.8

7. Conclusion

We have presented a mathematical analysis of macro-diversity gain that can be achieved in the LTE-A system. We have derived intra-cell and inter-cell interference models for LTE-A. A mathematical analysis of SINR gain with soft handover is carried out based on the MRC reception. The results show that propagation parameters significantly affect the choice of the handover margin and the SINR performance. We also presented system-level simulation results for selection of handover margin and the CoMP set size. The results in this paper can be used as a guideline in designing and optimizing the radio network based on LTE-A technology to improve the cell edge user performance. An analysis of handover gain for other deployment scenarios including heterogeneous networks will be the subject of future research.

References

- [1] 3GPP TR 36.814 V1.1.1, "Further Advancements for E-UTRA-Physical Layer Aspects," June 2009.
- [2] 3GPP TS 36.331 V8.2.0, "Evolved Universal Terrestrial Radio Access (E-UTRA) Radio Resource Control," 2008.
- [3] A.J. Viterbi, A.M. Viterbi, K.S. Gihousen, E. Zehavi, "Soft handoff extends CDMA cell coverage and increase reverse link capacity," *IEEE Journal On Selected Areas In Communications*, vol. 12, pp. 1281-1288, Oct. 1994. [Article \(CrossRef Link\)](#)
- [4] A.J. Viterbi, A.M. Viterbi, E. Zehavi, "Other-Cell Interference in Cellular Power-Controlled CDMA," *IEEE Trans. on Communications*, vol. 42, pp. 1501-1504, 1994. [Article \(CrossRef Link\)](#)
- [5] D. Wong, T.J. Lim, "Soft Handoffs in CDMA Mobile Systems," *IEEE Personal Communications*, vol. 4, pp. 6-17, Dec. 1997. [Article \(CrossRef Link\)](#)
- [6] K.M. Rege, S. Nanda, C.F. Weaver, W.C. Peng, "Analysis of Fade Margins for Soft and Hard Handoffs," in *Proc. of IEEE International Symposium on Personal, Indoor and Mobile Radio Communications (PIMRC 95)*, vol. 2, pp. 829-835, Sep. 1995.
- [7] H. Lee, H. Son, S. Lee, "Semisoft Handover Gain Analysis Over OFDM-Based Broadband Systems," *IEEE Trans. on Vehicular*, vol. 58, pp. 1443-1453, Mar. 2009.
- [8] C. Mihailescu, X. Lagrange, P. Godlewski, "Soft handover Analysis in Downlink UMTS WCDMA System," in *Proc. IEEE MoMuC*, pp. 279-285, 1999.
- [9] Jung Ah C. Lee, "Coordinated Multi-Point transmission in 3GPP LTE-Advanced," in *Proc. The 24th international conference on circuits/ systems, computers and communications*, Jeju, Korea, 2009.
- [10] R1-091687, "Discussion on the Relation between CoMP Cooperating Set and CoMP Reporting Set", NEC, 3GPP TSG-RAN WG1 57, May, 2009.
- [11] K.I. Pedersen, T.E. Kolding, F. Frederiksen, I.Z. Kovacs, D. Laselva, P.E. Mogensen, "An Overview of Downlink Radio Resource Management for UTRAN Long-Term Evolution," *IEEE Comm. Magazine*, vol. 47, pp. 86-93, 2009. [Article \(CrossRef Link\)](#).
- [12] Andrew J. Viterbi, "CDMA: Principles of Spread Spectrum Communication," Addison-Wesley Pub. Co., 1995.
- [13] Andrea Goldsmith, "Wireless Communications," Cambridge University Press, 2005.



Gun-Yeob (Peter) Kim received the B.S. and M.S. degrees in Electronics Engineering from Kyungpook National University, Korea. Currently he is with Alcatel-Lucent, Murray Hill, New Jersey. He is currently working towards the Ph.D. degree at the Department of Electrical and Computer Engineering, Stony Brook University - SUNY, Stony Brook, New York. Before joining Alcatel-Lucent, he worked at Samsung Electronics in Korea as a Senior Engineer and also worked at Willtech, Irvine, CA, as a Director. His research interests include mobility management and performance evaluation of cellular communication system.



Jung Ah C. Lee received the B.S. and M.S. degrees in Electronics Engineering from Seoul National University, Seoul, Korea. From 1992 to 1997, she was a research assistant at the Coordinated Science Laboratory, University of Illinois at Urbana-Champaign, where she received the Ph.D. degree in Electrical and Computer Engineering. Her thesis topic was on image formation algorithms for Synthetic Aperture Radar. Currently, she is with Alcatel-Lucent in Murray Hill, New Jersey, and has an appointment as an adjunct professor from the Stony Brook University - State University of New York, Stony Brook, NY. She is engaged in advanced signal processing algorithm, system design and performance analysis of 3G (UMTS/WiMAX) and 4G (LTE) cellular communication systems. She has actively contributed to 3GPP LTE standards in the area of Radio Access Technology. Her recent research interests are multiple antenna technology, radio resource management algorithm, and geo-location for cellular communication systems. She is the author of numerous papers and awarded and pending patents. She is the recipient of 2004 Bell Labs President's Gold Award for her contributions to 3GPP UMTS standardization.



Sangjin Hong received the B.S and M.S degrees in EECS from the University of California, Berkeley. He received his Ph.D. in EECS from the University of Michigan, Ann Arbor. He is currently with the department of Electrical and Computer Engineering at Stony Brook University – SUNY, Stony Brook, NY. Before joining SUNY, he has worked at Ford Aerospace Corp. Computer Systems Division as a systems engineer. He also worked at Samsung Electronics in Korea as a technical consultant. His current research interests are in the areas of low power VLSI design of multimedia wireless communications and digital signal processing systems, reconfigurable SoC design and optimization, VLSI signal processing, and low-complexity digital circuits. Prof. Hong served on numerous Technical Program Committees for IEEE conferences. Prof. Hong is a Senior Member of IEEE.